Testing of Optical System Based on Point Light Source

Xu Jingwei[1,2]　Yan Feng[1]　Zhang Xuejun[1]

([1] *Key Laboratory of Optical System Advanced Manufacturing Technology, Changchun Institute of Optics, Fine Mechanics and Physics, Chinese Academy of Sciences, Changchun, Jilin* 130033, *China*
[2] *University of Chinese Academy of Sciences, Beijing* 100049, *China*)

Abstract We introduce a simple method primarily developed for the performance evaluation of assembled space telescope in the field. The main idea of this method is to obtain the large parallel light beam for testing with an internal point light source and a plane mirror instead of large collimator. The wavefront error of the system can be calculated with phase diversity algorithm according to two images of the internal point source. The residual error and limitations of this method are discussed. A simulation is given at last, which shows the utilization potentiality of this approach.

Key words optical design; imaging systems; testing; optical systems; space optics system
OCIS codes 220.4840; 120.4820; 350.6090

应用点光源检测光学系统

许竞伟[1,2]　闫　锋[1]　张学军[1]

([1]中国科学院长春光学精密机械与物理研究所 光学系统先进制造技术重点实验室，吉林 长春 130033
[2]中国科学院大学，北京 100049)

摘要 介绍了一种简单的用于在外场检测空间光学系统的方法，其主要原理是通过内置点光源和外部的平面镜使系统自身产生平行光从而代替大口径平行光管。通过相位差异(PD)算法可以从点光源的图像中反演得出系统的波相差。讨论了该方法的限制。给出了仿真结果，证明了该方法的实用性。

关键词 光学设计；成像系统；检测；光学系统；空间光学系统
中图分类号 O435　　**文献标识码** A　　**doi**：10.3788/LOP50.122203

1 Introduction

A collimator is always applied to test space telescope after the imaging sensor is assembled[1-2]. However, as the aperture size and focal length of these systems become larger, it will be more difficult to test the system in the field considering that the difficulties of making and moving large collimator increase. Furthermore, it is also difficult to keep the environment condition steady in the field for optical testing. In this paper, a simple method for testing space telescopes in the field is proposed, in which the parallel light beam is produced by the telescope itself and the matched collimator is not needed any more[3].

2 Basic theory

The basic setup is shown in Fig. 1. A point light source is integrated on the component of focal plane array (FPA) and is used to generate the ideal spherical wavefront. The source should be assembled in the same plane of photosensitive surface of imaging sensor. The ideal spherical wavefront (the broken lines in Fig. 1) propagating into the system becomes plane wavefront (the real lines) after passing through the system. A plane mirror is located just in front of the aperture to reflect the parallel beam back into the system. The distance between the plane mirror and the aperture of optical system should be as short as possible to avoid

收稿日期：2013-08-29；**收到修改稿日期**：2013-09-08；**网络出版日期**：2013-11-12

作者简介：许竞伟(1991—)，男，硕士研究生，主要从事光学系统测试方面的研究。E-mail：fxkxjw@mail.ustc.edu.cn
导师简介：张学军(1968—)，男，研究员，博士生导师，主要从事先进光学制造技术方面的研究。E-mail：zxj@ciomp.ac.cn

the effect of airflow as much as possible. The reflected beams can be focused on the FPA by adjusting the orientation of the plane mirror. Therefore the image of the point light source is obtained. The small CCD settled beside the point light source is an assistant component for self-calibration of which the details will be expressed in latter parts. The small CCD should be placed close to the point light source as near as possible. Both the point light source and the small CCD should be located within the available field range of the system.

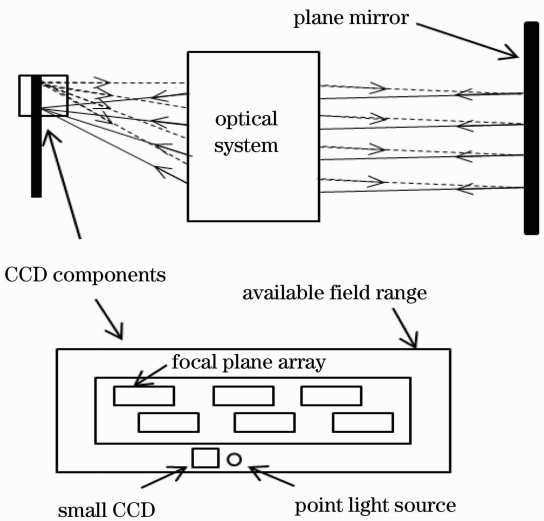

Fig. 1 Theoretical setup of the measurement

The wavefront error (WFE) along with the image of the point light source can be calculated through the phase diversity (PD) technique[4-8]. Phase diversity technique needs to collect two images while the first image is in focus containing the unknown WFE of the system, and the second image is diversity image which has an additional aberration. The additional aberration is specially designed and usually considered to be realized as defocusing. It is obvious that the light beams emitting from the point light source pass through the system twice, but follow different paths. Thus can be divided into two parts:

$$w = w_1 + w_2, \tag{1}$$

where w_1 stands for the WFE of the wavefront passing through the system the first time and w_2 stands for the WFE of the wavefront passing through the system the second time. In fact w_2 is just the WFE of the system what is indeed concerned about and w_1 can be regarded as a reference, because w_1 remains constant since the point light source is settled still so that the path of the incident light cannot be changed. Thus, if w_1 is measured, w_2 can be obtained.

w_1 can be measured by self-calibration with the assistant of the small CCD mentioned above. The small CCD can obtain the image of the point light source by adjusting the orientation of the plane mirror properly. In this case the incident and reflected light beams share almost the same path. The uncommon error depends on the distance between the point light source and the assistant CCD and the distance between the plane mirror and the stop of the optical system. The shorter both the two distances are, the less the uncommon error is. However, the effect of the uncommon error is very little in most cases. Take an $F/9$ Cook three-mirror anastigmatic (TMA) system for example. When the distance between the point light source and the assistant CCD is set 20mm and the distance between the plane mirror and the stop of the TMA system is set 1700 mm, the difference introduced by the uncommon error between w_1 and w_2 is only about 0.003λ with λ being the light wavelength. Such a difference is actually very small relative to the WFE of system and has little effect on the testing result. Hence it can be regarded approximately that w_1 equals w_2 without losing accuracy and

$$w_1 \approx w_2 \longrightarrow w = 2w_1 \longrightarrow w_1 = w/2. \tag{2}$$

After w_1 is calibrated, WFEs of different fields of view (FOVs) (w_2) can be obtained by adjusting the orientation of the plane mirror to make the image of point light source on corresponding CCD pixels and subtracting w_1 from the calculated WFE (w).

3 Limitation analysis

However, there is a problem in this method that the aperture of FOV under test is limited by the aperture

stop of the optical system, which is mainly because the incident light beams and the reflected light beams follow different paths, as shown in Fig. 2. It can be easily deduced that the spot of reflected beams on the stop of system cannot overlap with that of incident beams because they have the same cross-section area but stand for different FOVs. Therefore only the WFE of the overlapping area (part B) can be obtained while the WFE of other area will be lost.

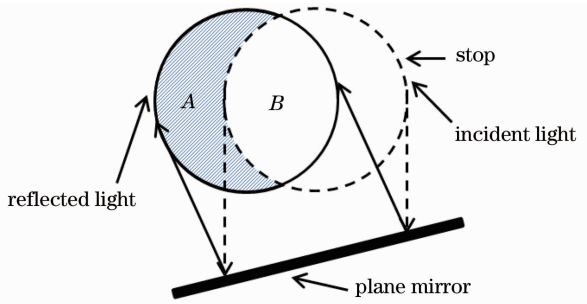

Fig. 2 Diagram of the incident and reflected rays on the stop where the circle in broken line stands for the spot on the stop of incident light, and the real line represents that of reflected light

The limitation of testing area is not all the same for different systems. As mentioned above, decreasing the distance between the system and the plane mirror can enlarge the effective area for testing by shortening the optical paths. Narrow FOV can also help to reduce the negative effect of the limitation. Take Rug-TMA system for instance. The stop is located at the position of primary mirror and the FOV of such a system is always narrow, as shown in Fig. 3(a), so that the plane mirror can be set just in front of the primary mirror so long as keeping a safe distance to the barrel. Hence the lost area is always very small. But for a Cook-TMA system, the stop is located at the position of secondary mirror and the FOV in one direction is usually very wide, as shown in Fig. 3(b), and the effective testing area of the widest FOV will be relatively small. The percentage of the overlapping area to the full aperture is corresponding to the parameters of different systems. It can achieve more than 80% even for the widest FOV of most usual telescopes. The detailed analysis is omitted for length consideration and will be given elsewhere.

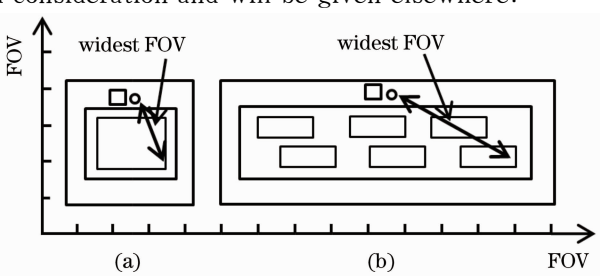

Fig. 3 FOVs of (a) Rug-TMA system and (b) Cook-TMA system

One solution to this problem is to settle several pairs of point light source and small CCD at different locations around the FPA of the system, as shown in Fig. 4. For any given FOV under test, the nearest pair of point light source and small CCD can be selected to minimize the path difference and maximize the overlapping area. Another solution is to make the point light source and small CCD mobile along a trail, which can move to the most proper position for different FOVs under test. Both methods are under consideration and detailed implementation will be given in future work.

Finally, it must be pointed out that the limitation of testing area is not a fatal drawback of this method. What is most concerned about in outdoor testing is the global low-order WFE, which is caused by mechanical

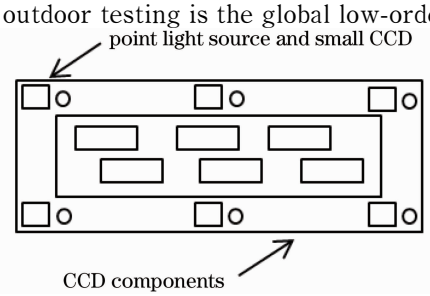

Fig. 4 Solution to full aperture test

stress, thermal stress, etc., but not the local high-order WFE. This low-order WFE can be abstracted from a large sub-aperture (the overlapping area) without losing accuracy, while the full-aperture testing is encouraged but not so necessary.

4 Simulation result

Simulation is established basically through Zemax and Matlab. Zemax is used for generating both the in-focus and the defocusing images of a simulated point light source and Matlab is used for extracting the WFE through phase diversity algorithm. The theoretical WFE is set as the reference as shown in Fig. 5. A circle area is selected from the overlapping area for convenience of mathematical processing[9]. Figure 5(a) is the sum WFE of the incident and the reflected wavefronts, and Fig. 5(b) is the theoretical WFE of the reflected wavefront, which is 0.0220λ. The calculated results are shown in Fig. 6. Figure 6(a) is the sum WFE of the incident and the reflected wavefronts, and Fig. 6(b) is the WFE of the reflected light, which is 0.0237λ.

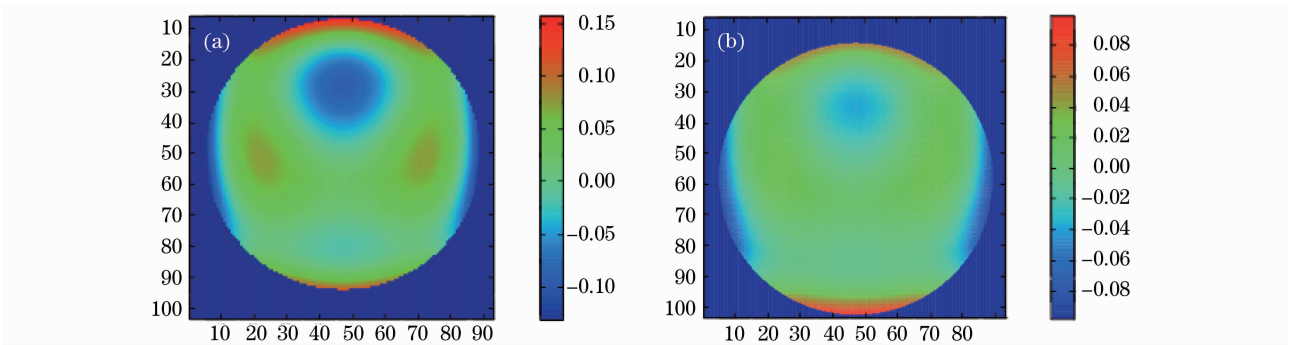

Fig. 5 Theoretical results. (a) Sum WFE of the incident and the reflected wavefronts; (b) WFE of the reflected wavefront, 0.0220λ (λ = 632.8 nm)

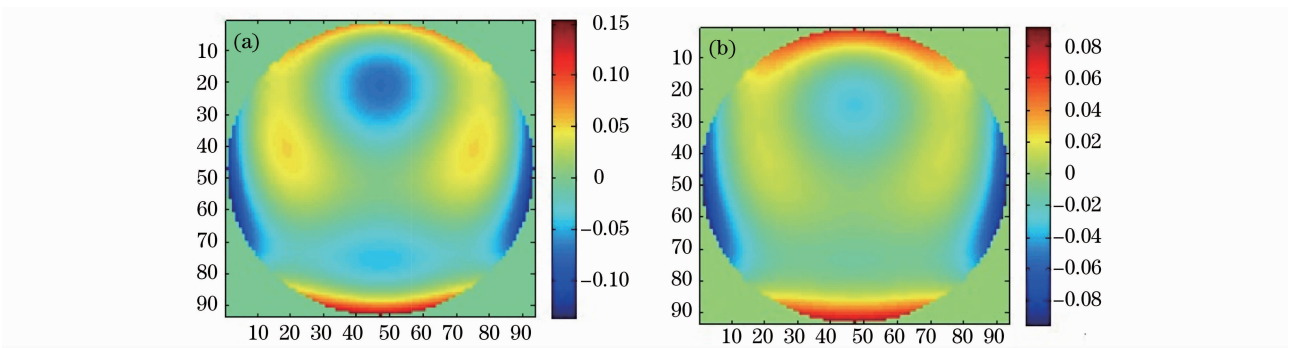

Fig. 6 Calculated results. (a) Sum WFE of the incident and the reflected wavefronts; (b) WFE of the reflected wavefront, 0.0237λ (λ = 632.8 nm)

The difference between the theoretical WFE and the calculated WFE is only 0.0016λ, as shown in Fig. 7. This difference is caused mainly by the uncommon optical paths between the incident wavefront and the reflected wavefront as well as other factors. However, the calculated results are still encouraging since the difference is small compared with the real WFE. So this measurement is proved to be applicable. Practical experiment is under preparation.

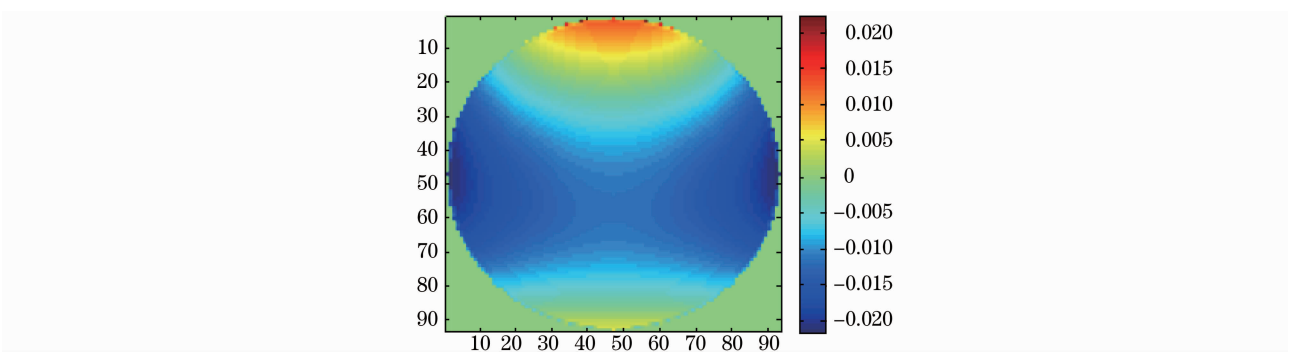

Fig. 7 Difference between WFE of the theoretical wavefront and the calculated wavefront

Applying this method in outdoor testing, the environment factors which may have negative effects on taking images need to be considered, e.g., the temperature and air turbulence. In common conditions, temperature changes very slowly and has little influence on the result. Air turbulence can cause much difference to the taken images. However, since the image collection and data processing are very quick, the additional error caused by air turbulence can be removed through comparing several different groups of results. The CCD used in this measurement is the same as that of the system and the entire testing process is highly efficient. So in common conditions, the consistency of CCD is well accepted.

5 Conclusion

A new method for testing space telescope out of laboratory is described. The fundamental setup of this measurement only consists of a point light source, a small CCD around the FPA and a plane mirror, which is effective and convenient to be carried out. Although full aperture WFE cannot be obtained, the calculated WFE is enough for performance evaluation. The difference between the theoretical result and the calculated result is small and the testing accuracy is acceptable. The detailed analysis and the practical experiment will be given in the future.

References

1 S B Hutchison, A Cochrane, S McCord, *et al*.. Updated status and capabilities for the LOTIS 6.5 meter collimator[C]. SPIE, 2008, 7106, 710618.

2 R M Bell, G C Robins, C Eugeni, *et al*.. LOTIS at completion of collimator integration[C]. SPIE, 2008, 7017, 70170D.

3 M Gai, D Busonero, A Riva. A metrology concept for multiple telescope astrometry[C]. SPIE, 2012, 8442, 84421O.

4 D J Lee, M C Roggemann, B M Welsh, *et al*.. Evaluation of least-squares phase-diversity technique for space telescope wavefront sensing[J]. Appl Opt, 1997, 36(35): 9186 - 9197.

5 Cheng Qiang, Yan Feng, Xue Donglin, *et al*.. Wavefront error testing of off-axis three-mirror anastigmatic system using phase diversity technology[J]. Chinese J Lasers, 2012, 39(10): 1008001.
程 强,闫 锋,薛栋林, 等. 利用相位差异技术检测离轴三反光学系统的波前误差[J]. 中国激光, 2012, 39(10): 1008001.

6 Liang Shitong, Yang Jianfeng, Xue Bin. A new phase diversity wave-front error sensing method based on genetic algorithm [J]. Acta Optica Sinica, 2010, 30(4): 1015 - 1019.
梁士通,杨建峰,薛 彬.基于遗传算法的改进相位差法波前误差传感技术研究[J]. 光学学报, 2010, 30(4):1015 - 1019.

7 Wang Xin, Zhao Dazun. Influence of noise to phase diversity wavefront sensing[J]. Acta Optica Sinica, 2009, 29(8): 2142 - 2146.
王 欣,赵达尊. 图像噪声对相位变更波前传感器的影响研究[J]. 光学学报,2009,29(8): 2142 - 2146.

8 Yang Huizhen, Gong Chenglong. Phase retrieval for a kind of wavefront sensor based on pupil phase diversity[J]. Acta Optica Sinica, 2011, 31(11): 1112002.
杨慧珍,龚成龙. 一种基于瞳面相位差的波前传感器相位恢复[J]. 光学学报, 2011, 31(11): 1112002.

9 D Malacara. Optical Shop Testing (3rd edition)[M]. New York: Wiley, 2007. Chap. 13.